Two-Dimensional Mapping of the Electrostatic Potential in Transistors by Electron Holography

W. D. Rau,[1] P. Schwander,[1] F. H. Baumann,[2] W. Höppner,[1] and A. Ourmazd[1]
[1]*Institute for Semiconductor Physics, Walter-Korsing-Strasse 2, 15230 Frankfurt (Oder), Germany*
[2]*Bell Laboratories, Lucent Technologies, 600 Mountain Avenue, Murray Hill, New Jersey 07974*
(Received 28 August 1998)

We demonstrate the first successful mapping of the two-dimensional electrostatic potential in semiconductor transistor structures by electron holography. Our high resolution 2D phase maps allow the delineation of the source and drain areas in deep submicron transistors. By measuring the mean inner potential of Si and surface depletion effects in thin cross-section samples, we have directly determined the 2D electrostatic potential distribution with 10 nm spatial resolution and 0.1 V sensitivity. We discuss the sensitivity limits of the technique, and outline its possible applications in the study of solid state reactions in two dimensions within a few nanometers of the surface. [S0031-9007(99)08770-0]

PACS numbers: 85.40.Qx, 61.16.Bg, 85.30.–z, 85.40.–e

Within a decade, integrated circuits may consist of transistors as small as 150 atoms long and 50 atoms deep. In an economically viable process technology, no more than 64 of the 50 billion transistors printed on a single chip are allowed to fail [1]. Transforming this "road map" into reality presupposes unprecedented control of a number of key solid state processes, and constitutes one of the most exciting challenges facing modern solid state science.

Fundamentally, a silicon transistor is a highly inhomogeneous distribution of precisely placed dopants. It is thus remarkable that, up to now, no technique exists to map the distribution of dopants in transistors in two dimensions [2]. The dopant distribution must thus be inferred via a complex procedure. First, the solid state processes used to fabricate the device, such as implants, anneals, etches, etc., are simulated to "fabricate a virtual device." Next, the electrical characteristics of the virtual device are simulated and compared with measurements from the actual device. Iterative corrections are made in the process models until an agreement is reached. The actual dopant distribution is then assumed to be giving the best agreement between the simulated and measured electrical characteristics.

The importance of having a direct method capable of mapping 2D dopant distributions has long been recognized [3]. Scanning capacitance microscopy (SCM) has produced compelling images [4], which, unfortunately, depend sensitively on the tip and the applied voltage. SCM images are thus difficult to translate into dopant maps without substantial modeling. In various pioneering works, electron holography has been used to map electric fields in pn junctions [5–8]. The state of the art has so far indicated "the promise of this technique for measuring potential distributions across device junctions" [9].

Here, we demonstrate the first successful mapping of the 2D depletion region electrostatic potential in deep submicron transistors with 10 nm resolution and 0.1 V sensitivity. Our primary results can be summarized as follows. (a) The source and drain regions can be directly imaged in n- and p–metal-oxide-semiconductor transistors (n- and p-MOSFETs, [10]), with the appropriate sign and magnitude of the potential change [11]. (b) Because of surface depletion effects, thin cross-section samples suitable for electron holography have a 25-nm-thick "dead layer" at each surface, within which the potential distribution is not representative of the bulk. (c) The optimum sample thickness for mapping the potential distribution in silicon is 200–400 nm. This is determined by a trade-off between the phase shift of the electron wave propagating through the sample and inelastic scattering. Both of these effects increase with sample thickness, but have opposite effects on the sensitivity. (d) We place an upper limit of 5.9 nm on any differential thinning across pn junctions in our electron transparent samples, corresponding to an accuracy of 0.24 V in the potential measurement. In the absence of any differential thinning, or when the thickness change across the junction is known, other sources of noise limit the sensitivity to 0.1 V in potential.

Taken together, our results transform electron holography into a practical tool for quantitatively mapping 2D dopant distributions in predetermined microscopic regions of materials with high spatial resolution and sensitivity.

We now outline the basic principle of the approach. An electrostatic potential distribution induces a local phase shift in a plane electron wave passing through an electron transparent sample [6–8]. For a sample containing a pn junction with its plane oriented along the beam direction, and under experimental conditions that minimize dynamical diffraction effects [12], the phase shift is given by

$$\varphi = C_E[V_0 t + \Delta V_{pn}(t - 2t_0)]. \quad (1)$$

C_E is an interaction constant [12,13], V_0 the mean inner potential corresponding to the index of refraction for electrons [12], and t the sample thickness. Because of surface depletion effects on the top and bottom of the thin cross-section samples, the effective sample thickness contributing to the pn junction signal is reduced by t_0 at

 0031-9007/99/82(12)/2614(4)$15.00

each surface. The depletion region potential ΔV_{pn} can be extracted from a measurement of φ, provided V_0, t, and t_0 can be measured. We use off-axis electron holography in a transmission electron microscope (TEM) to measure interferometrically the local phase of an electron wave that has passed through the sample of interest. V_0 and t_0 are measured in test samples with known dopant distributions and geometries. The phase images can then be translated into maps of depletion region electrostatic potential.

The experimental details are as follows. We use a Philips CM200 Lorentz TEM operating at 200 kV equipped with a field-emission gun and an electron biprism. The amplitude and phase of the modulated exit wave $A(x, y)e^{i\varphi(x,y)}$ are measured by interference with a reference wave that has passed through vacuum only [6–8]. The samples consisted of submicron transistors in silicon (100), prepared as ⟨110⟩ cross sections by conventional mechanical polishing and low-angle Ar milling. Wedge-shaped test and calibration samples containing abrupt *pn* junctions were also prepared by focused ion beam milling. Samples were viewed about 4° off the ⟨110⟩ zone axis to minimize dynamical diffraction effects [9,14].

Conceptually, we determine ΔV_{pn} as follows. First, we map the phase φ in a wedge-shaped reference sample of a known wedge angle and plot φ vs t (thickness). The slope of this plot gives V_0 [Eq. (1)]. Then, we plot the phase change $\Delta\varphi_{pn} = C_E \Delta V_{pn}(t - 2t_0)$ across a *pn* junction of a reference sample vs thickness and determine $2t_0$ from the intercept with the t axis. A map of the phase in a sample of interest can then be translated to a map of ΔV_{pn} across the *pn* junction through Eq. (1). In practice, it is important to use more sophisticated methods to exploit the available information efficiently, and to determine whether there are differential thinning effects across the *pn* junction. Such thickness changes can mimic, or hide ΔV_{pn}, the change in the potential due to the *pn* junction (see below).

We now show that our approach clearly reveals *p*- and *n*-submicron MOS transistor structures in unprocessed electron phase images. Figure 1 shows amplitude and phase images of 0.35 μm channel length *n*- and *p*-MOSFET transistors. The source and drain areas are clearly visible in the phase images and, as expected, show contrast reversal between *n*-MOS (As doped) and *p*-MOS (B doped) devices. The spatial resolution is better than 10 nm.

We now describe how such phase images can be translated into maps of the electrostatic potential. The approach consists of using reference samples to obtain the mean inner potential V_0 and the thickness t_0 of the dead layer at each surface. Figures 2(a) and 2(b) show an electron hologram and a phase image, respectively, obtained from a wedge-shaped reference sample containing a *pn* junction [15]. The wedge angle was measured to be 29.5° ± 0.6° from thickness contour images obtained in bright field at the zone axis. In an Argand diagram, the

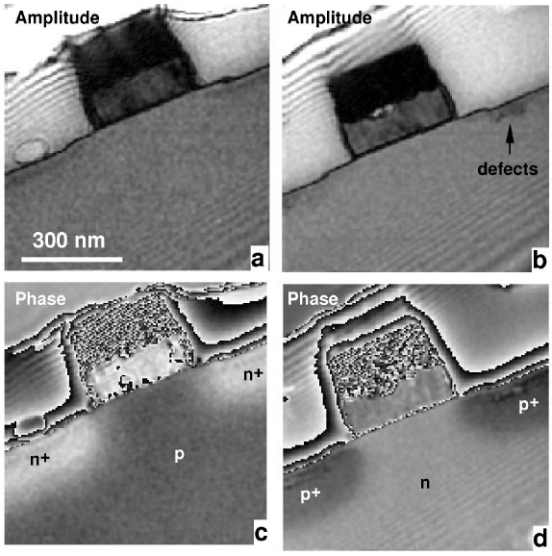

FIG. 1. Amplitude and phase images of 0.3 μm *n*-MOS (left) and *p*-MOS (right) transistors, viewed in cross section. The source and drain areas (marked as n^+ or p^+) are clearly visible in the phase images with the appropriate contrast. Abrupt black-white contrast lines are due to phase changes larger than 2π. The location of defects near the original wafer surface can be measured with respect to the extension of the source/drain areas.

measured complex electron wave $A_0 e^{-b\varphi} e^{i\varphi}$ sweeps out a logarithmic spiral [Fig. 3(a)]. The damping b of the spiral is due to increasing inelastic scattering with thickness and is proportional to the ratio between the absorption potential and $V_0 + \Delta V_{pn}$ [16]. For a known wedge angle, V_0 can be directly measured from the path rate $d\varphi/dt$ in a plot of φ vs t [Eq. (1), [14]]. Our measurements yield a value of 11.9 ± 0.7 V for V_0. The uncertainty is due mainly to the errors in the determination of the wedge angle and the exact electron optical magnification [17].

We now turn to determining t_0, the thickness of the dead layer at each sample surface. Figure 3(b) is a plot of the electron phase change $\Delta\varphi_{pn}$ across the *pn* junction vs thickness for a reference sample, prepared in the same way as the transistor structures. The intercept with the t axis yields a value of 49.0 ± 3.3 nm for $2t_0$ [18].

Armed with experimental values for V_0 and t_0, we are now in a position to translate phase images of deep submicron transistor structures into maps of the electrostatic potential change ΔV_{pn}. A phase image of a 0.18 μm long transistor is shown in Fig. 4(a) [19]. Figure 5 is the electrostatic potential distribution across the 0.18 μm *p*-MOSFET. We believe this constitutes the first 2D map of the electrostatic potential *inside* device structures obtained at high spatial resolution and sensitivity. We measure a drop in depletion region potential of 0.9 ± 0.12 Vacross the *pn* junction. This is within one sigma of the theoretical value of 1.02 V for the given dopant levels.

We place an upper limit on any differential thinning effects across the junction as follows. We fit the damping

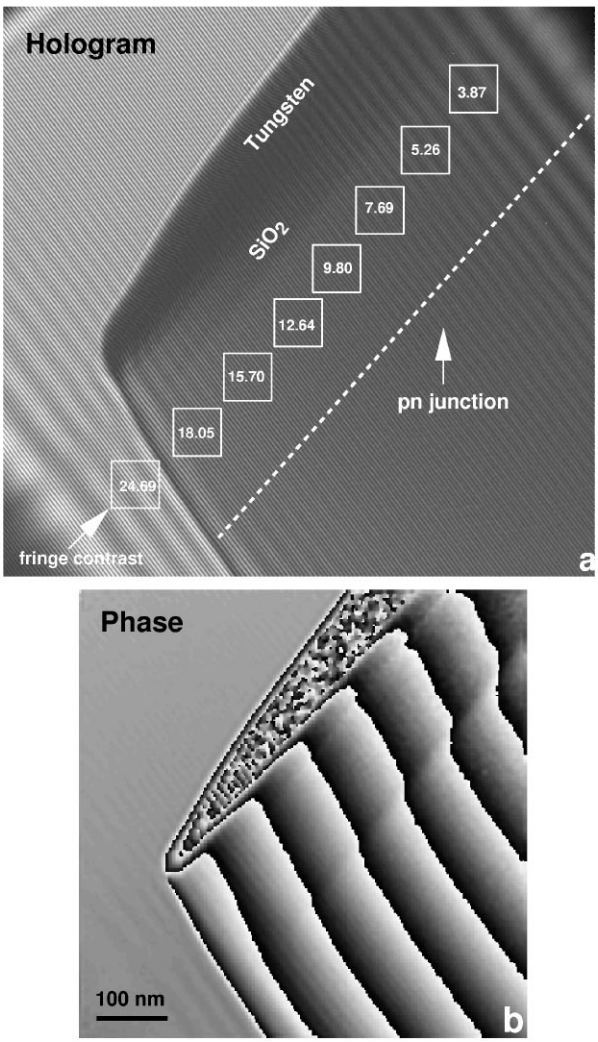

FIG. 2. (a) Hologram of a wedge-shaped sample containing an abrupt *pn* junction. The position of the *pn* junction is arrowed. The contrast of the hologram fringes is reduced with increasing thickness as indicated. (b) Reconstructed phase image. The phase signal across the *pn* junction increases with thickness. A minimum thickness is needed to reveal the junction.

term b of the spiral path [Fig. 3 (a)] in regions of constant potential in the sample. Since the damping is inversely proportional to $V_0 + \Delta V_{pn}$, a change in attenuation due to the potential difference can be revealed. We note that this approach is independent of the local thickness. We measure a difference in b across the junction, corresponding to a change of $(7.65 \pm 2.1)\%$ in the total potential, in good agreement with the value of 7.56% deduced from the phase change across the *pn* junction. By translating the error into a thickness change, an upper limit of 5.9 nm for differential milling across the *pn* junction can be extracted. This corresponds to an upper limit of 0.24 V for the error in ΔV_{pn} due to any systematic differential thinning effects.

We now discuss the issues concerning the practical application of this technique and its ultimate sensitivity.

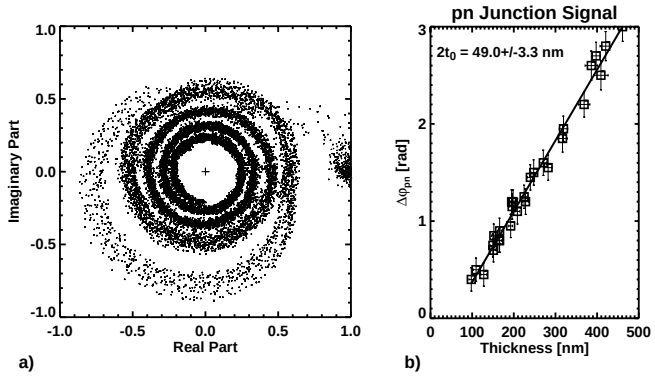

FIG. 3. (a) Argand plot of the complex wave from Fig. 2. The experimental data points sweep out a logarithmic spiral. The damping of the spiral is due to inelastic scattering. (b) Relative phase change $\Delta\varphi_{pn}$ across the *pn* junction versus sample thickness. An extrapolation to zero phase shift yields the thickness t_0 of the dead layer at each surface.

Several important observations may be made from Fig. 2. (a) With increasing sample thickness, the fringe contrast in the hologram is reduced due to incoherent inelastic scattering [7,8]. (b) The phase shift at the *pn* junction increases linearly with thickness. (c) A minimum sample thickness is needed to reveal the junction. These three effects combine to produce an optimum thickness for electrostatic potential mapping. We have measured these effects, including the reduction in the holographic fringe contrast with thickness, and determined the change in the sensitivity of electrostatic field mapping with sample thickness [Fig. 4(b)]. For Si, the optimum thickness lies in the range 200–400 nm. With the present electron optical parameters, a sensitivity of 0.1 V can be reached (for a detailed discussion, see [7]).

We now speculate on the broader implications of our work. It should now be possible to use electron holography to study dopants and their interactions in microscopic, near-surface regions of solids. Specifically, the

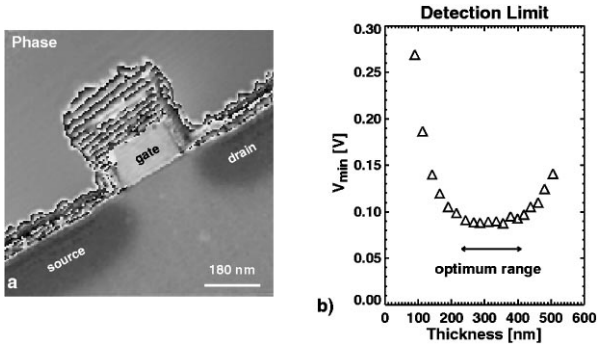

FIG. 4. (a) Phase image of 0.18 μm channel length *p*-MOS transistor. (b) Minimum detectable depletion region potential $\Delta V_{\min}$ versus specimen thickness. An optimum thickness regime between 200 and 400 nm for potential mapping is apparent.

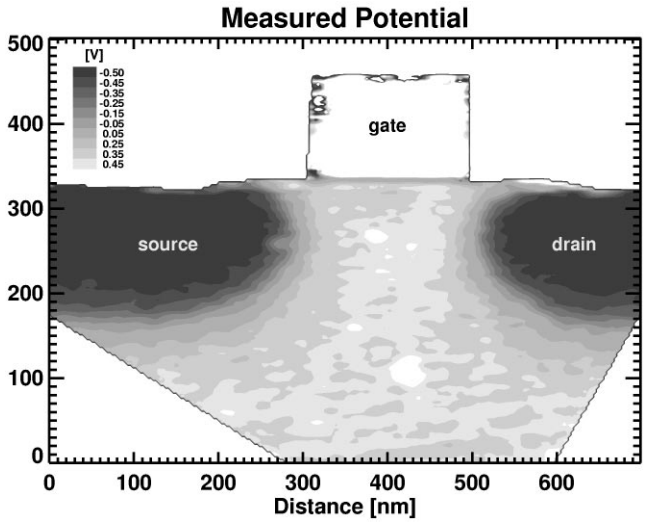

FIG. 5. Map of the depletion region potential extracted from the phase image of Fig. 4. The electrostatic potential changes by 0.9 ± 0.12 V across the *pn* junction.

study of complex diffusion phenomena in the highly inhomogeneous structures used in modern technology appears within reach. This should expedite the development of physically based process simulators with genuine predictive power, so urgently needed by fundamental and technologically relevant solid state science [20].

In summary, we have shown that electron holography can be used as a practical tool to map the two-dimensional electrostatic potential in deep submicron device structures with 10 nm spatial resolution and 0.1 V sensitivity.

We gratefully acknowledge H. Lichte and H. Banzhof for extensive discussions and access to their facilities. We also thank M. Gribelyuk, B. Heinemann, J.-L. Maurice, C. S. Rafferty, H. Rücker, and H.-H. Vuong for valuable contributions. The support of this work by the Volkswagenstiftung is gratefully acknowledged.

[1] *The National Technology Roadmap for Semiconductors,* SIA Semiconductor Industry Association (1998), http://www.sematech.org/public/roadmap/

[2] The two critical dimensions are the transistor length and depth.

[3] A. C. Diebold, M. R. Kump, J. J. Kopanski, and D. G. Seiler, J. Vac. Sci. Technol. B **14**, 196 (1996).

[4] R. N. Kleiman *et al.,* in *Proceedings of the IEDM Technical Digest International Electron Devices, 1997* (IEEE, Piscataway, NJ, 1997), p. 691.

[5] S. Frabboni, G. Matteucci, G. Pozzi, and M. Vanzi, Phys. Rev. Lett. **55**, 2196 (1985).

[6] A. Tonomura, Rev. Mod. Phys. **59**, 639 (1987).

[7] H. Lichte, in *Handbook of Microscopy,* edited by S. Amelinck, D. van Dyck, J. van Landuyt, and G. van Tendeloo (VCH Publ., Weinham, 1997).

[8] "Introduction to Electron Holography," edited by E. Voelkl, D. Joy, and L. Allard (Plenum Press, New York, to be published).

[9] M. R. McCartney *et al.,* Appl. Phys. Lett. **65**, 2603 (1994).

[10] The doping sequence for the source-channel-drain region of *n*- and *p*-MOSFETs is *npn* and *pnp*, respectively.

[11] The magnitude of the potential change measured in [9] (1.5 ± 0.2 V) is larger than the silicon band gap. This was ascribed to "anomolous contrast" from defects, surface pinning, etc.

[12] J. C. H. Spence, in *Experimental High Resolution Electron Microscopy* (Oxford University Press, New York, 1988), 2nd ed.

[13] $7.295\ 10^{-3}\ \mathrm{rad\,V^{-1}\,nm^{-1}}$ for the 200 keV electrons used throughout this work.

[14] M. Gajdardziska-Josifovska *et al.,* Ultramicroscopy **50**, 285 (1993).

[15] The sample was grown by chemical vapor deposition containing an abrupt *pn* junction ($1 \times 10^{19}\ \mathrm{cm^{-3}}$ B on $5 \times 10^{18}\ \mathrm{cm^{-3}}$ P), and prepared by focused ion beam (FIB) milling. The sample was covered by 35 nm SiO_2 and 100 nm of W, which acts as a protection layer during FIB preparation.

[16] M. R. McCartney and M. Gajdardziska-Josifovska, Ultramicroscopy **53**, 283 (1994).

[17] Despite the deviation from the published value of 9.3 V [14], more recent measurements indicate similar results [M. R. McCartney (private communication)].

[18] We note that t_0 depends on the doping level and sample preparation and has to be measured afresh for the samples of interest.

[19] Since TEM specimens are wedge shaped, a corresponding phase change determined by extrapolation from areas of constant doping level was subtracted. The local specimen thickness at the junction position is 282 ± 17 nm.

[20] W. D. Rau *et al.,* in *Proceedings of the IEDM Technical Digest International Electron Devices Meeting, 1998* (IEEE, Piscataway, NJ, 1998), p. 713.